NASA Technical Memorandum 84230

Computation of Incompressible, Three-Dimensional Turbulent Boundary Layers and Comparison With Experiment

U.R. Müller

May 1982

National Aeronautics and
Space Administration

NASA Technical Memorandum 84230

Computation of Incompressible, Three-Dimensional Turbulent Boundary Layers and Comparison With Experiment

U. R. Müller, Ames Research Center, Moffett Field, California

NASA
National Aeronautics and
Space Administration

Ames Research Center
Moffett Field, California 94035

COMPUTATION OF INCOMPRESSIBLE, THREE-DIMENSIONAL TURBULENT BOUNDARY LAYERS AND COMPARISON WITH EXPERIMENT

U. R. Müller*

NASA Ames Research Center

SUMMARY

The incompressible three-dimensional, turbulent boundary layer (3DTBL) experiments of van den Berg and Elsenaar (ref. 1), Dechow (ref. 2) and Müller (ref. 3) were simulated numerically by integrating the boundary-layer equations together with an algebraic eddy-viscosity turbulence model. For the flow treated by van den Berg and Elsenaar, the downstream portion, where the crossflow was large, could not be predicted with the present computational method; we feel that this flow was significantly influenced by elliptic flow-field effects. Though Dechow's experiment also indicated departures from the boundary-layer concept, our calculations agreed reasonably well with the mean-flow development up to separation. In Müller's experiment the normal pressure gradients were found to be negligible in regions with large skewing and enabled us to test turbulence models using the boundary-layer equations. The simulation of this flow compared favorably with the experimental data throughout the flow field and suggested the applicability of algebraic eddy-viscosity models for 3DTBLs.

INTRODUCTION

Predictions of 3DTBLs are needed for many engineering purposes, for example, in designing swept, low aspect ratio wings and improving their performance. However, the development of computational methods, as well as our understanding of the turbulent momentum transfer in three-dimensional flows, has lagged substantially behind the state of art reached for two-dimensional flows. Since only a small number of experiments was available, which documented both the mean flow field and the Reynolds stresses of 3DTBLs, turbulence modeling for such flows was not always confirmed experimentally. For most numerical computations of 3DTBLs, turbulence models developed for two-dimensional flows have been applied together with an ad hoc closure assumption for the crossflow momentum equation. The predictions of low speed flows with moderate crossflow generally compared well with experimental data, but flow fields with large crossflow often could not be simulated with reasonable accuracy (ref. 4), especially the flow field experiment performed by van den Berg and Elsenaar (ref. 1). Comparison computations for this experiment failed to predict the three-dimensional part of the flow ahead of separation. Several attempts have been made to improve the results of this experiment. Krause (ref. 5) and Kordulla, for example, investigated the applicability of several algebraic turbulence models, but found the results of the computations to be strongly coupled with the numerical accuracy and also with the accuracy with which the outer-edge boundary conditions

*National Research Council Associate

were prescribed. Since isotropic turbulence models assume equal directions of the resultant, turbulent shear stress vector and the rate-of-strain vector throughout the flow field, Rotta (ref. 6) used the measurements of Elsenaar and Boelsma (ref. 7), to develop an anisotropic closure assumption for the pressure-strain correlation and obtained slight improvement of the predictions. From the same set of measurements Cousteix et al. (ref. 8) developed a heuristic transport equation for the direction of the shear stress vector; their computations also indicated some improvements of the results only. Rubesin's computations as discussed in reference 9, used a closure model for the transport equations of the Reynolds stresses and did not require an a priori assumption for the degree of anisotropy, but again for the three-dimensional flow region only small improvements were achieved compared to the other calculations. All predictions mentioned so far did not only underestimate the development of the secondary flow, but also failed to predict separation. The latter could only be enforced under modified conditions like those of Elsenaar et al. (ref. 10), who increased the prescribed pressure distribution and also reduced the influence of the turbulence model by adjusting several coefficients to the experimental data.

Based on the results of 3DTBL simulations like those mentioned above, Marvin (ref. 9) suggested that eddy-viscosity turbulence models may not be adequate for computing flows with severe crossflow but need considerable improvement. The present author feels that further comparisons of measured and predicted mean-flow and turbulence fields are needed before discarding simple, gradient-diffusion turbulence models. In fact, during the recent years several documentations of 3DTBL developments including the measurements of all components of the Reynolds stress tensor were completed, for example by Dechow (ref. 2) and Müller (ref. 3). To the author's knowledge these experiments have not yet been used for comparing theory and experiment.

In the present study the three flow fields were simulated numerically by solving the boundary-layer equations. We concentrated our efforts on investigating whether an algebraic turbulence model as developed for two-dimensional flows allows for reasonable predictions of 3DTBLs. In order to sort out the applicability of a particular turbulence model, we also had to study the sensitivity of the predictions to modifications of the closure assumptions and to the accuracy of the pressure distribution prescribed.

NUMERICAL METHOD AND TURBULENCE MODELS

The equations for incompressible 3DTBLs were integrated in a Cartesian frame of reference:

$$\left.\begin{aligned} \partial\overline{U}/\partial x + \partial\overline{V}/\partial y + \partial\overline{W}/\partial z &= 0 \quad ; \quad \partial p/\partial y = 0 \\ \overline{U}\partial\overline{U}/\partial x + \overline{V}\partial\overline{U}/\partial y + \overline{W}\partial\overline{U}/\partial z &= -(1/\rho)\partial p/\partial x \\ &\quad + \partial(\nu\partial\overline{U}/\partial y - \overline{uv})/\partial y \\ \overline{U}\partial\overline{W}/\partial x + \overline{V}\partial\overline{W}/\partial y + \overline{W}\partial\overline{W}/\partial z &= -(1/\rho)\partial p/\partial z \\ &\quad + \partial(\nu\partial\overline{W}/\partial y - \overline{vw})/\partial y \end{aligned}\right\} \qquad (1)$$

Quasi-two-dimensional flows were computed setting $\partial/\partial z = 0$; while for two-dimensional flows $\bar{W}$ was set to zero. The boundary conditions included no-slip conditions at the wall and prescribed outer-edge velocities, which were determined by smoothing the measured pressure distribution and solving the Euler equations. The baseline turbulence model used for closing equation (1) was formed by Michel et al.'s (ref. 11) mixing-length formula together with the assumption of isotropic eddy viscosities.

$$\left.\begin{aligned} -\overline{uv} &= \nu_x \partial\bar{U}/\partial y \quad ; \quad -\overline{vw} = \nu_z \partial\bar{W}/\partial y \quad ; \quad \nu_t = \nu_x = \nu_z \\ \nu_t &= \ell^2 F^2 \{(\partial\bar{U}/\partial y)^2 + (\partial\bar{W}/\partial y)^2\}^{\frac{1}{2}} \quad ; \quad F = 1 - \exp\{-y u_\tau N/(26\nu)\} \\ \ell/\delta &= \ell_e/\delta * \tanh\{0.41/(\ell_e/\delta)*(y/\delta)\} \quad ; \quad u_\tau = \sqrt{|\vec{\tau}_w|/\rho} \quad ; \quad \ell_e/\delta = 0.085 \end{aligned}\right\} \tag{2}$$

We applied Cebeci's (ref. 12) pressure gradient correction to the van Driest damper F with s being the coordinate along the outer-edge streamline:

$$N = (1 - 11.8\, p^+)^{\frac{1}{2}} \quad ; \quad p^+ = -\{1/(\rho u_\tau^3)\}\partial p/\partial s \quad . \tag{3}$$

Additionally, we used a closure assumption with anisotropic eddy-viscosities. As suggested by Rotta (ref. 6) the Reynolds stresses were defined in a local coordinate system, the x-axis of which was aligned with the yaw direction of the resultant flow vector. Then the stresses were transformed into the frame of reference used for equation (1).

$$\left.\begin{aligned} -\overline{u_m v_m} &= \tilde{\nu}_x \partial\bar{U}_m/\partial y \quad ; \quad -\overline{v_m w_m} = T\tilde{\nu}_z \partial\bar{W}_m/\partial y \quad ; \quad \tilde{\nu}_x = \tilde{\nu}_t \quad ; \\ \tilde{\nu}_z &= T\tilde{\nu}_t \quad ; \quad \tilde{\nu}_t = \ell^2 F^2 \{(\partial\bar{U}_m/\partial y)^2 + T(\partial\bar{W}_m/\partial y)^2\}^{\frac{1}{2}} \quad . \end{aligned}\right\} \tag{4}$$

The ratio T of the eddy viscosities defined the degree of anisotropy.

The initial conditions for the spanwise integration were obtained either from solving the plane-of-symmetry equations (ref. 12) or by integrating equation (1) with Hall's difference scheme. The CFL-condition was applied in the wall-streamline direction. Then the integration was carried out with Crank-Nicholson differencing. For all computations we used step sizes $\Delta x = \Delta z = 8$mm; the normal grid spacing Δy was smaller than $y^+ = 1$ at the wall and then was stretched towards the outer edge yielding 70 to 150 node points across the boundary layer. As found from test calculations, grid effects were negligible for all results obtained.

The integration of the governing equations was based on the algorithm of Krause et al. (ref. 13). Using the baseline turbulence model the computational method was tested against case A4 of reference 4 (turbulent boundary layer approaching a cylinder mounted perpendicular to the surface). As shown in figure 1, the results obtained for the turning angle β_w between outer-edge and wall streamline directions, and for the shape factor H evaluated with the streamwise velocity profile, agreed well with the predictions of other differential methods.

RESULTS OF NUMERICAL SIMULATIONS

Experiment of van den Berg et al. (Refs. 1, 7)

This investigation of a 3DTBL on a swept flat plate was performed under "infinite swept-wing conditions", that is vanishing gradients of all flow variables in spanwise direction, figure 2. By means of a diffuser-type channel an adverse pressure gradient normal to the leading edge was generated, such that three-dimensional separation occurred in the downstream region.

We obtained the initial conditions for starting the numerical simulations by matching a two-dimensional, zero-pressure gradient, turbulent boundary-layer calculation with Reynolds number $Re = 2.42 \times 10^6$ ($\bar{U}_\infty$ defined at station 1; L = 1m) to the measured momentum-thickness Reynolds number and skin friction coefficient. Then a small crossflow yielding $\beta_w = 1.5^\circ$ was prescribed according to reference 1.

The computation of the downstream flow development was carried out under quasi-two-dimensional conditions with $\partial/\partial z = 0$. Using the pressure distribution measured at the wall together with the baseline turbulence model we obtained the result indicated by (run A1) in figures 3 and 4. Up to station 5 the measured and calculated mean velocity profiles as well as the skin friction coefficients $c_f = 2\bar{\tau}_w/(\rho\bar{U}_e^2)$ and the wall turning angles $(\alpha+\beta_w)$ agreed well. The angle α defined the direction of the outer-edge flow with respect to the x-axis. Further downstream the comparison indicated deviations which increased rapidly; at station 7 the computed wall turning angle lagged 15° behind the measured value of 40°, while the mean velocity component $\bar{U}$ was overpredicted as much as 100% in the near-wall region. The spanwise velocity $\bar{W}$ was obtained a few percent too large. Beyond station 7 the computed values of c_f and β_w were approximately constant and did not lead to separation. These results were identical to those reported earlier, for example by Krause (ref. 5). Carrying out a fully three-dimensional calculation by using the corresponding wall pressure distribution of reference (1), we did not observe any improvements in the predicted results. When using a standard turbulence model the calculation was insensitive to the departures from the ideal infinite swept wing case.

In the three-dimensional flow at station 7 the Reynolds shear stresses $\overline{u_m v_m}$ and $\overline{v_m w_m}$ acting in the local yaw direction and normal to it, respectively, indicated peak values at 12 mm $\lesssim$ y $\lesssim$ 15 mm, which were 25 to 30% higher than those of the experimental data. Since in the outer layer the calculated mean velocity gradients were evaluated smaller than the measured ones, these results seemed to indicate an overestimation of the turbulent viscosities by the closure assumption used. That is why we reduced the magnitude of viscous forces in subsequent calculations. First we considered Rotta's definition of anisotropic eddy viscosities, equations (4). In reference 7 the ratio of the local crosswise to streamwise viscosity was measured as $0.5 < T < 0.6$ upstream of station 5 and as $T \geqslant 0.7$ downstream of this station. According to Müller's (ref. 14) error analysis for turbulence measurements in 3DTBLs, accurate results for this ratio are very difficult to obtain, especially in weak three-dimensional flows. That is why for the present calculations the ratio T was set equal to one initially and then was gradually reduced beyond station 4 or 5, respectively, such that the prescribed experimental value was obtained at the next downstream measuring station. In our calculation with T = 0.7, introduced at station 5, we found negligible differences compared to run A1.

Cousteix et al. (ref. 8) applied $T < 1$ throughout the flow field; their computations yielded, for example, overestimated turning angles in the flow region with moderate crossflow and then seemed to improve the results slightly in the three-dimensional part.

Second, we investigated the sensitivity of the results to the mixing-length distribution prescribed. While in reference 7 the measured inner-layer lengths scales were close to $\ell = 0.41y$, the normalized outer-layer data approached $\ell_e/\delta = 0.07$ at station 5 and 0.05 at station 7; thereby they deviated significantly from the distribution assumed by the baseline model. Plotting the mixing length distributions $\ell(y)$, however, indicated that these profiles were approximately constant downstream of station 4 or 5 and did not scale with the boundary-layer thickness δ. "Freezing" the length scale distribution at one of these stations effectively was identical to the empirical relationship of Elsenaar et al., reference 10, $\ell_e/\delta \tilde{\alpha} (1-\overline{V}_e)$ where $\overline{V}_e$ is the normal velocity at the outer edge. When using equation (2) up to station 5 and then "freezing" $\ell(y)$, the results were close to those of run A2, figure 3. For run A2 $T = 0.7$ was used in addition to the frozen mixing length. Downstream of station 6 the skin friction coefficient decreased slightly with increasing x-coordinate, while between stations 7 and 8 β_w was 5° higher than in run A1. Again, separation was not predicted.

In further computations we investigated the sensitivity of the predictions to the prescribed static pressure distribution. In reference 1 the pressure at the outer edge of the boundary-layer was derived from the mean-flow measurement and was found to be larger than that at the wall downstream of station 6. For our test calculations we assumed a pressure rise between stations 6 and 7 leading to a value that was 2% higher than the one measured at the wall. The downstream outer-edge pressure data were approximated by a polynomial curve fit. The approximation of the outer-edge data as indicated by the broken line in figure 2 will be used throughout the calculations discussed hereafter. Using the baseline turbulence model the results indicated an increase in β_w by 4°, while c_f stayed about the same. However, when we applied the larger pressure distribution together with the reduced eddy viscosities of run A2, we obtained a monotonic decrease of c_f (run A3 in figure 3) and separation occurred between stations 9 and 10. At station 7 the spanwise velocity $\overline{W}$ agreed well with the experimental data, figure 4, while the velocity component $\overline{U}$ was still overpredicted. The turbulent shear stress profiles decreased considerably compared to the previous runs; except for a narrow region close to the wall they were smaller than in the experiment. Introducing $T = 0.7$ at station 4 had little effect compared to run A3 where $T = 0.7$ was introduced at station 5.

For run A4 we used isotropic eddy viscosities and kept the mixing length distribution constant downstream of station 4; then we also introduced $T = 0.7$ at the same station, run A5. Compared to previous computations c_f decreased further, and β_w increased substantially. For run A5 β_w even indicated an overshoot compared to the measurements, while both mean velocity components were close to the experimental data. For this case the momentum thickness, defined with the streamwise velocity profile in the direction of the resultant outer-edge velocity, was evaluated at station 7 as 5.95 mm compared to the experimental value of 6.35 mm (5.06 mm in run A1), while the shape factor $H = 1.65$ was identical to the experimental value (1.45 in run A1). At the same station the peaks in the profiles of both Reynolds shear stresses $u_m v_m$ and $v_m w_m$ were about 30 percent below the measured ones.

Dechow's Experiment (Ref. 2)

Dechow investigated a 3DTBL approaching a tear-drop shaped body extending between lower wall (test surface) and upper wall of a channel with a height of 300 mm, figure 5. Most measurements of mean velocities and Reynolds stresses were taken at stations oriented along an external streamline. Since the present computational method was limited to attached flows, we could not simulate any measurements downstream of station 6. The two-dimensional initial conditions at $x = 0$ were obtained from smoothing the measured velocity profile $\overline{U}(y)$ of station 1. We matched the momentum thickness Reynolds number and the skin friction coefficient to the experimental data. The free-stream Reynolds number was prescribed as 1.45×10^6 with $\overline{U}_\infty$ defined at station 1 and $L = 1m$. The computations discussed below were based on the measured wall pressure distribution displayed in figure 6. Our curve fit by means of cubic splines approximated the measurements well, but we encountered problems in obtaining smooth distributions of the pressure gradients, especially for the downstream region of the flow, where too few measurements have been carried out. Therefore using the plane-of-symmetry solution as starting conditions for the crosswise integration (applied for case A4 of reference 4, see fig. 1) was not sufficiently accurate, but generated large oscillations of all flow quantities. The profile of the normal velocity $\overline{V}$ at the first location off the plane of symmetry $z = \Delta z$ indicated a strong flow acceleration resulting in negative velocities $\overline{V}$. This indicated that the profiles of $\partial\overline{W}/\partial z$ calculated at $z = 0$ with $\partial^2 p/\partial z^2$ and the crosswise pressure gradient prescribed at $z = \Delta z/2$ were not compatible. Maybe smaller step sizes Δz close to the plane of symmetry would have removed this problem. Instead we solved the boundary-layer equations with Hall's scheme in the vicinity of the plane of symmetry. Since in that region the near-wall turning angle of the flow was small, we shrank the computational domain with $\tan^{-1}(\Delta z/\Delta x) = 3°$. In test runs we reduced the computational domain with $\tan^{-1}(\Delta z/\Delta x) = 30°$ downstream of $x = 350$ mm and found negligible effects. The downstream side boundary of the computational domain was prescribed with $z = 128$ mm.

The results obtained from calculations with the baseline turbulence model are indicated by solid lines in figures 7 to 10. Up to station 4 the inner-layer profile of the mean velocity $\overline{U}$, figure 7, agreed well with the experimental data, while the outer-layer profile was underpredicted by about 10% at station 4. Further downstream the near-wall flow was predicted to be larger than the measurements suggesting that for this part of the flow the turbulent viscosities were overestimated by equation (2). Indeed, at stations 5 and 6 the measured mixing length distributions could not be represented by $\ell = 0.41\, y$ anymore but were much less. The mean velocity component $\overline{W}$ was obtained close to the experimental data except for the outer layer of the profiles farthest downstream where the calculations were a few percent too large. The momentum thicknesses defined with the streamwise velocity profile in the direction of the outer-edge flow were found to be up to 10% higher than in the measurements. The calculated shape factor H was 5% larger than the experimental value at station 3 ($H = 1.48$), was close to the measurements at station 4 and 5 ($H = 1.47$; $H = 1.52$), but about 7% smaller at station 6 ($H = 1.56$). At $x = 500$ mm and $z = 50$ mm a shape factor larger than 1.8 indicated incipient separation, which, in fact, occurred immediately downstream of this cross-section ($x = 508$ mm and $z \approx 44$ mm). In figure 8 the calculated Reynolds shear stresses $\overline{u_m v_m}$ and $\overline{v_m w_m}$ are compared with the experimental data. In the outer layer the predicted $\overline{u_m v_m}$ correlation generally was too large. While at station 3 the peak value was only slightly higher than in the experiment, the maximum was too high by 20% at station 5 and 25% at station 6. The measured Reynolds stresses $\overline{v_m w_m}$ were not well represented by the computations; as for the van den Berg et al. experiment they were considerably overestimated. However, the magnitude of this shear stress was much smaller than that

of the streamwise component (less than 1/4 up to station 4), and its effect on the mean flow development was expected to be fairly small. Additionally, the near-wall measurements tend to be smaller than zero. Such results are not compatible with mixing length theory and indicate severe experimental uncertainties.

At stations 3 and 4 (x = 350 mm and 425 mm) the computed skin friction coefficients as displayed in figure 9, were smaller than the Preston tube measurements by 4% or 7%, respectively, while at station 5 (x = 475 mm) they were 10 percent larger. Since at station 6 the measured mean velocity profile defined in the direction of the near-wall flow, could not be described by the law of the wall anymore, the measurement is probably in error. In figure 9 we have also included the results of computations for the plane of symmetry, where two additional measurements were available. From the oil flow pattern of reference 2 we extracted several spanwise distributions of the wall turning angle, figure 10. We found good overall agreement even in the strong crossflow region except very close to separation (x = 500 mm and z < 65 mm).

In additional computations we investigated the sensitivity of the predictions to the prescribed turbulent length scale distribution. The experimental results did not indicate the outer layer similarity presumed by equation (2), but yielded $\ell_e/\delta = 0.07$ up to station 4 and $\ell_e/\delta = 0.06$ further downstream. Approximating the measurements by a fixed length scale $\ell_e = 2.4$ mm we obtained the results displayed by broken lines in figures 7 to 10. The profiles of the mean velocity component $\bar{U}$ indicated considerably smaller velocities in the near-wall region. Correspondingly, the flow separated ahead of station 6 already. The magnitude of the Reynolds shear stress $u_m v_m$ was considerably reduced, and the profiles were close to the experimental data. The crosswise shear stress only indicated a minor sensitivity. Corresponding to the mean-velocity profiles, the wall shear stresses were predicted lower than in the baseline computation (approximately by 0.00015 for $x \geq 350$ mm). The wall turning angle was close to the previous run up to x = 425 mm. At x = 475 mm the results were 5° larger at z_{max}, but were 25° larger at z_{min} and indicated incipient separation.

As investigated by further test calculations (not shown), we found that the predicted near-wall flow quantities in the region close to separation significantly depended on the prescribed pressure distribution, which was measured to be larger at the wall than at the outer edge for $x \geq 350$ mm. Using the latter data together with the baseline turbulence model yielded a constant spanwise distribution of β_w at x = 500 mm, and the flow separated further downstream compared to the results obtained with the wall pressure distribution.

Generally, our numerical simulation of Dechow's experiment yielded reasonable overall agreement with the measured mean-flow profiles and wall quantities even in the strong crossflow region with turning angles at the wall of about 30°. However, similar to the experiment of van den Berg et al., the present one also indicated upstream pressure disturbances caused by flow separation on the test surface and probably enhanced by displacement effects of the flow at the upper-wall of the channel. Again, pressure gradients in the direction normal to the wall were present and thus impaired comparison calculations carried out by means of the boundary-layer equations.

Müller's Experiment (Ref. 3)

In this experiment a 3DTBL on a flat plate was generated by laterally deflecting the initial flow, figure 11. The static pressure distribution measured at the outer edge of the boundary layer is displayed in figure 12. We obtained a good representation of the pressure field except for $z > 500$ mm by approximating the measurements by polynomial functions of fourth order. At five z-coordinates the distribution of $c_p(x)$ was evaluated and then, at arbitrarily prescribed x-coordinates, the crosswise distributions $c_p(z)$ were computed. To save computer time and because we did not encounter problems in calculating two-dimensional flows or those with moderate crossflow, we did not start the numerical simulations at $x = 0$ but at $x = 140$ mm instead. At each crosswise grid point the smoothed velocity profile of station B5 was normalized by the magnitude of the measured outer-edge flow and was assumed to be collateral to the outer-edge velocity vector. With this starting procedure we obtained velocity profiles at $x = 200$ mm, which differed less than 3% from the measurements, see, for example, profile B5 in figure 13. The lateral boundaries of the computational domain were defined by $z_{max} = 600$ mm and by a wall streamline starting at $x = 140$ mm and $z = 84$ mm, while x_{max} was prescribed with 650 mm.

In figures 13 to 16 the measured downstream development of the flow is compared with the computed one obtained with the baseline turbulence model. For all stations with $z = 500$ (row 5) the profiles of the mean velocity component $\overline{U}$ were in close agreement with the measurements, figure 13, while the peaks in the profiles of the $\overline{W}$ component were underpredicted by about 10%. Close to the separation line, at stations D2 and E3, the agreement was noticeably worse. For $z = 500$ mm the momentum thicknesses evaluated for the streamwise profiles were found to be about 6% smaller than the experimental values. Since the displacement thicknesses were also underpredicted, the shape factors did not deviate more than 2% from the measurements ($H = 1.46$ at station E5 and $H = 1.48$ at station F5).

The computed and measured Reynolds stresses $\overline{u_m v_m}$ and $\overline{v_m w_m}$ are compared in figure 14. Generally, good overall agreement was obtained for the streamwise component. The deviations for $y \lesssim 5$ mm at the upstream stations were probably caused by experimental inaccuracies. The profiles of the measured shear stress $\overline{v_m w_m}$ developed peaks at $y \approx 7$ mm which were not obtained from the computations and were underestimated by as much as 30% at station E5 and 50% at station E3. However, since in the near-wall region the gradients of the computed crossflow velocities were underpredicted also, we could not expect closer agreement of measurements and predictions. In the outer layer the comparison yielded satisfactory results.

The computed skin friction coefficients based on the total wall shear stresses are displayed in figure 15. For $x > 200$ mm the agreement was good except for $z > 500$ mm, where the outer-edge pressure distribution had been prescribed too high. At $x = 600$ mm the differences between measurements and computations increased with decreasing distance from separation and were as high as 15% at z_{min}. In figure 16 the directions of the resultant wall shear stresses, computed at the measuring stations, are compared with the wall flow visualization. Excluding the results at stations close to separation and those for $z > 500$ mm, the agreement was good, particularly since the crossflow angles β_w were as high as 40°. Generally, the results obtained from the numerical simulation of this experiment indicated that except for the region close to separation the downstream development of this flow was predicted well.

CONCLUDING REMARKS

Numerical simulations of the 3DTBL-experiments of van den Berg and Elsenaar (ref. 1), Dechow (ref. 2) and Müller (ref. 3) were carried out in order to test the applicability of an algebraic mixing length turbulence model in flows with strong crossflow. Additional to the baseline integrations of the boundary-layer equations we also investigated the sensitivity of the predictions to modification of the turbulence model or to the prescribed outer-edge boundary conditions. Generally, for the regions with moderate skewing ($\beta_w < 15^\circ$) the flow-field calculations agreed well with the experimental data. For the highly three-dimensional parts of the flows, however, we found different degrees of agreement for each case.

The computed downstream development of the flow measured by van den Berg and Elsenaar failed to simulate the measurements. Separation was only obtained if the pressure distribution prescribed was larger than the one measured at the wall and simultaneously the magnitude of the eddy viscosities was reduced compared to the baseline model; this was also true in the computations of Elsenaar et al. (ref. 10). Under these conditions the results proved to be extremely sensitive to either modification; for example, changing the pressure distribution by a few percent yielded large changes in the computed flow field. We feel that the problems encountered were these conditions the results proved to be extremely sensitive to either modification; for example, changing the pressure distribution by a few percent yielded large changes in the computed flow field. We feel that the problems encountered were mainly a result of the breakdown of the boundary-layer concept in the downstream part of the flow. Though in the experiment the diffuser cross-section approximately varied linearly throughout the flow field, the longitudinal pressure gradients rapidly decreased beyond station 5. This upstream pressure effect was caused by separation and the flow blockage at the downstream end of the diffuser. Additionally, pressure variations normal to the wall probably influenced the development of this flow. For resolving these elliptic flow-field effects, predicting the location of separation and ultimately testing turbulence models, a Navier-Stokes prediction method would be necessary.

Our numerical simulation of Dechow's experiment yielded reasonable overall agreement with the measured mean-flow profiles and wall quantities even in the strong crossflow region with turning angles of about 30° between wall- and outer-edge flow direction. However, the flow field close to separation was found to be sensitive to the pressure distribution prescribed, as well as to the turbulence model used. In the three-dimensional flow, the measurements indicated normal pressure gradients which impaired the comparison with solutions of the boundary-layer equations. Additionally, in the downstream part of the flow similarity laws as developed for two-dimensional mean flow and turbulence fields were not valid anymore. Under these conditions we could not extract detailed information about turbulence modeling.

In Müller's experiment, which was performed in a wind tunnel with an open test section of 1 m Ø, most measuring stations were located at sufficiently large distances away from separation in order to ensure negligible normal pressure gradients. The results of the numerical simulation for this flow indicated a minor dependency on the accuracy of the prescribed pressure distribution and enabled us to study the applicability of the turbulence model used. Except for the region closest to separation, the flow development, computed with a baseline turbulence model, compared favorably with the measurements even at the measuring stations farthest downstream with large skewing ($\beta_w > 40^\circ$). In contrast to the other calculations, the results were found to be insensitive to the outer-layer mixing length and suggested the applicability of an algebraic eddy-viscosity model as developed for two-dimensional

boundary layers. In order to fully understand the results obtained, further investigations with more sophisticated turbulence models will be necessary, which take into account the experimentally observed anisotropy of the turbulence field or the normal Reynolds stress diffusion, respectively.

The present study again demonstrates the lack of well-documented experiments which are suitable to guide both the development of computational methods for 3DTBLs and closure assumptions as well. Because pressure forces play a dominant role in flows like those investigated here, future experiments should accurately map out the pressure distribution and also ensure that the boundary layer concept is valid. Based on such experiments we expect progress in turbulence modeling for 3DTBLs as well as in the development of prediction methods for engineering-type applications.

REFERENCES

1. van den Berg, B.; Elsenaar, A.: Measurements in a Three-Dimensional Incompressible Turbulent Boundary-Layer in an Adverse Pressure Gradient Under Infinite Swept Wing Conditions. NLR TR 72092 U, 1972.

2. Dechow, R.: Mittlere Geschwindigkeit und Reynoldsscher Spannungstensor in der dreidimensionalen Wandgrenzschicht vor einem stehenden Zylinder. In: Strömungsmechanik und Strömungsmaschinen, Mitteilungen des Institutes für Strömungslehre und Strömungsmaschinen, Heft 21 (1977), Univ. Karlsruhe.

3. Müller, U. R.: Measurement of the Reynolds Stresses and the Mean Flow-Field in a Three-Dimensional Pressure-driven Boundary Layer. J. Fluid Mech. 119 (1982), 121.

4. East, L. F.: Computation for Three-Dimensional Turbulent Boundary Layers. FFA TN AE-1211, 1975.

5. Krause, E.: Strive for Accuracy-Improvement of Predictions. Comp. and Fluids 8 (1980), 31.

6. Rotta, J. C.: A Family of Turbulence Models for Three-Dimensional Thin Shear Layers. In: 1st Symposium on Turbulent Shear Flows, Pennsylvania State Univ., 1977.

7. Elsenaar, A.; Boelsma, S. H.: Measurements of the Reynolds Stress Tensor in a Three-Dimensional Turbulent Boundary-Layer under Infinite Swept Wing Conditions. NLR TR 74095 U, 1974.

8. Cousteix, J.; Aupoix, B.; Pailhas, G.: Synthese de Resultats Theoriques et Experimentaux sur les Couches Limites et Sillages Turbulents Tridimensionnels. ONERA-NT-1980-4, 1980.

9. Marvin, J. G.: Turbulence Modeling for Computational Aerodynamics. AIAA paper 82-0164, 1982.

10. Elsenaar, A.; van den Berg, B.; Lindhout, J.P.F.: Three-Dimensional Separation of an Incompressible Turbulent Boundary-Layer on an Infinite Swept Wing. AGARD-CP-168, 1975.

11. Michel, R.; Quémard, C.; Durant, R.: Application d'un Schéma de Longeur de Mélange à l'Étude des Couches Limites Turbulentes d'Équilibre. ONERA TN 154, 1969.

12. Cebeci, T.: Calculation of Three-Dimensional Boundary-Layers II. Three-Dimensional Flows in Cartesian Coordinates. AIAA J. 13 (1975), 1056.

13. Krause, E.; Hirschel, E. H.; Bothmann, Th.: Differenzenformeln zur Berechnung dreidimensionaler Grenzschichten. DLR FB 69-66, 1969.

14. Müller, U. R.: On the Accuracy of Turbulence Measurements with Inclined Hot Wires. J. Fluid Mech. 119 (1982), 155.

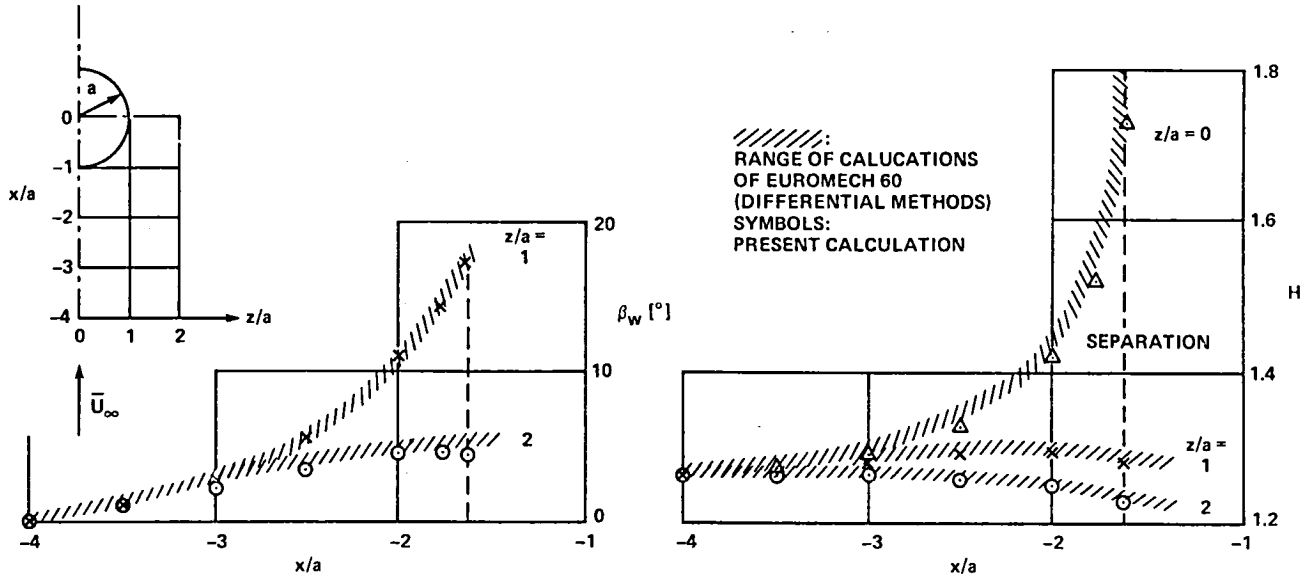

Figure 1. - Comparison of calculated wall turning angles and shape factors with with computations of reference 4.

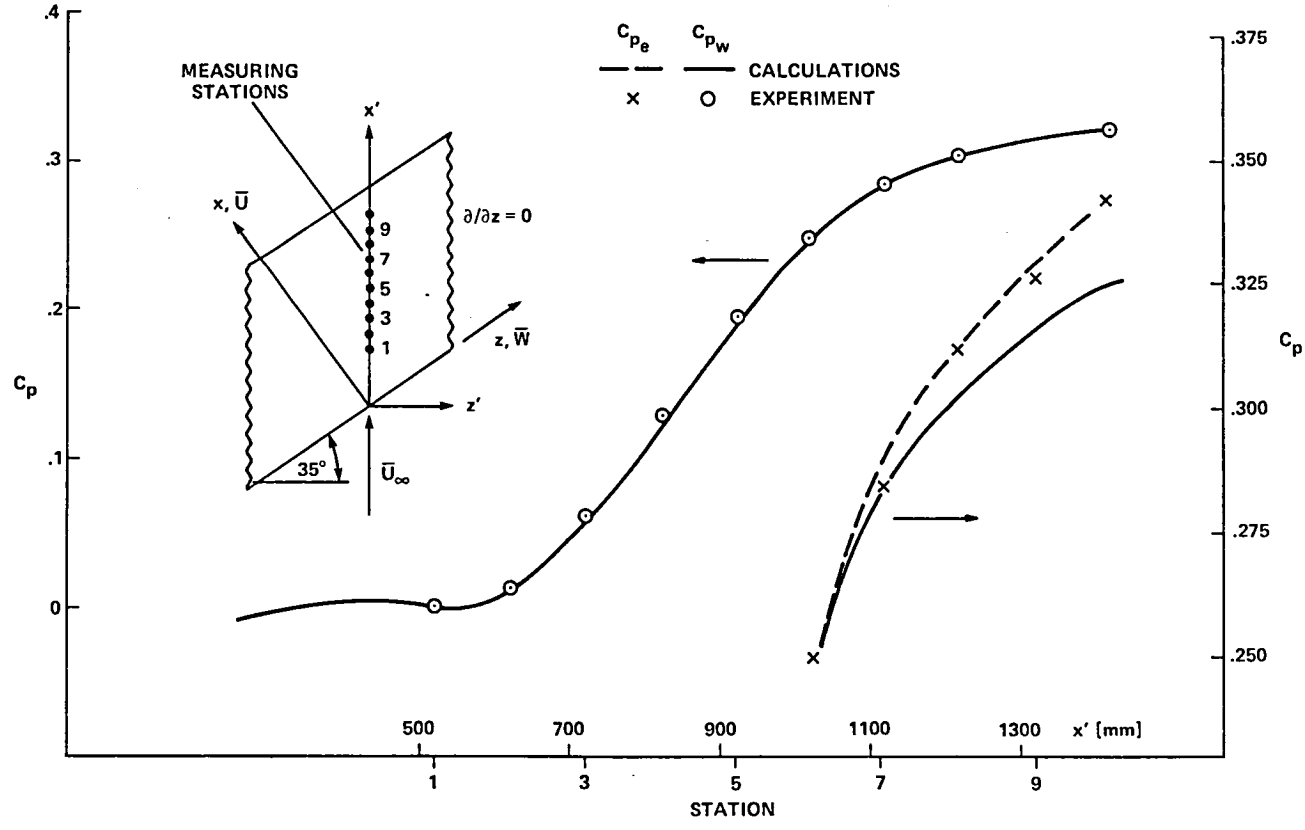

Figure 2. - Experimental setup of reference 1 and pressure distribution.

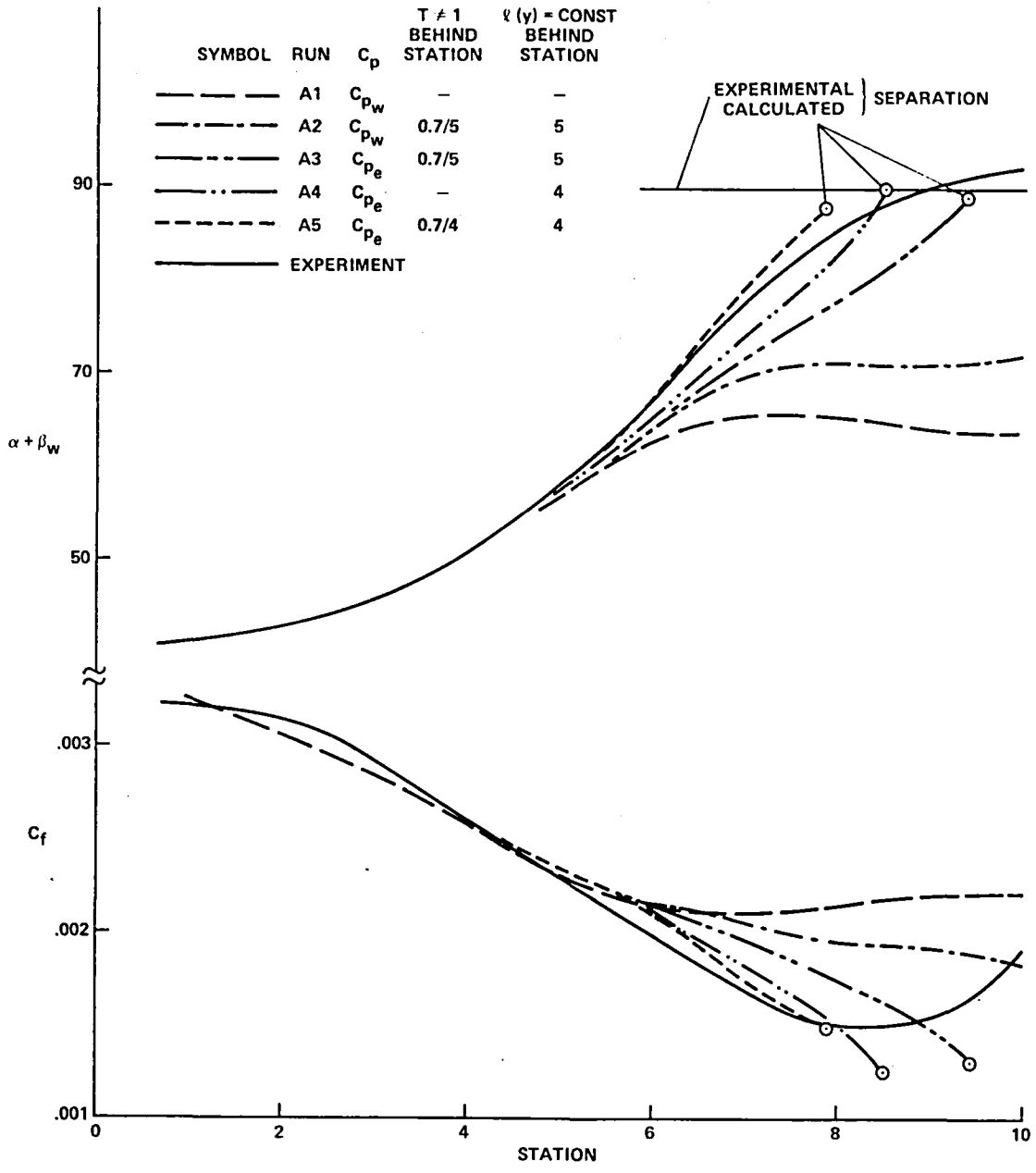

Figure 3. - Comparison of measured and computed wall turning angles and skin friction coefficients for different eddy viscosities and pressure distributions.

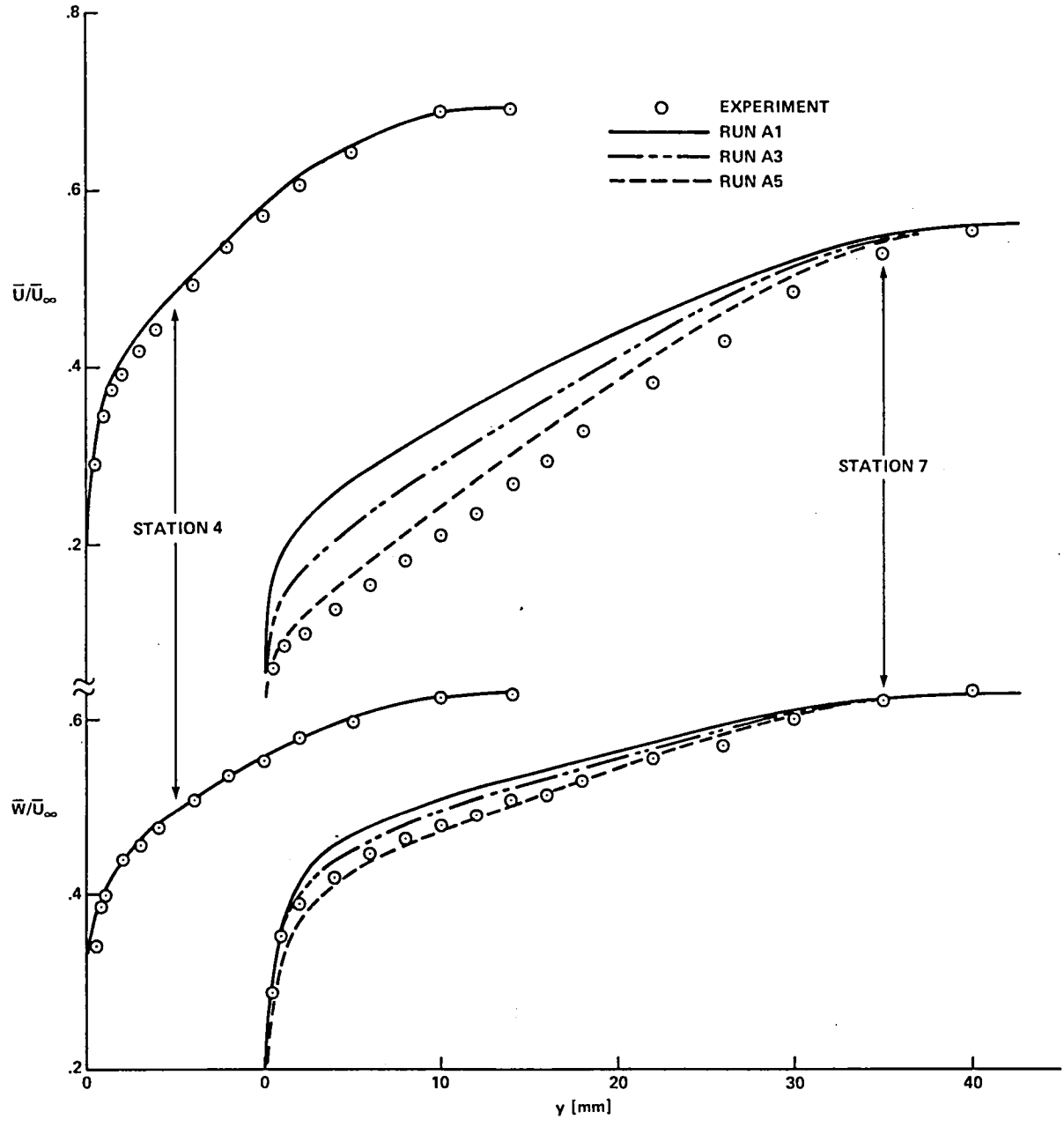

Figure 4. - Comparison of measured and computed mean velocities.

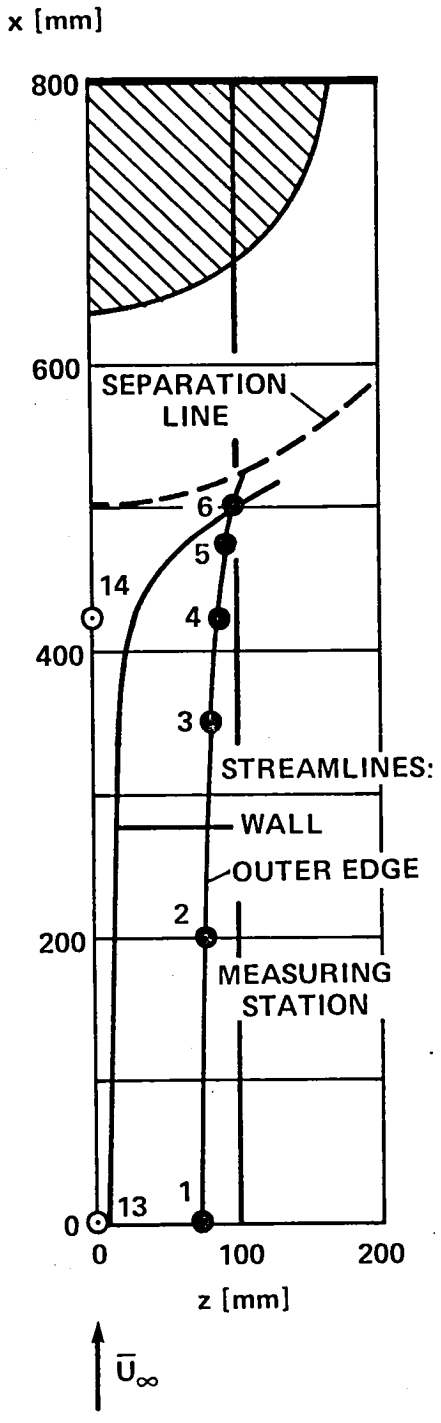

Figure 5. - Experimental setup of reference 2.

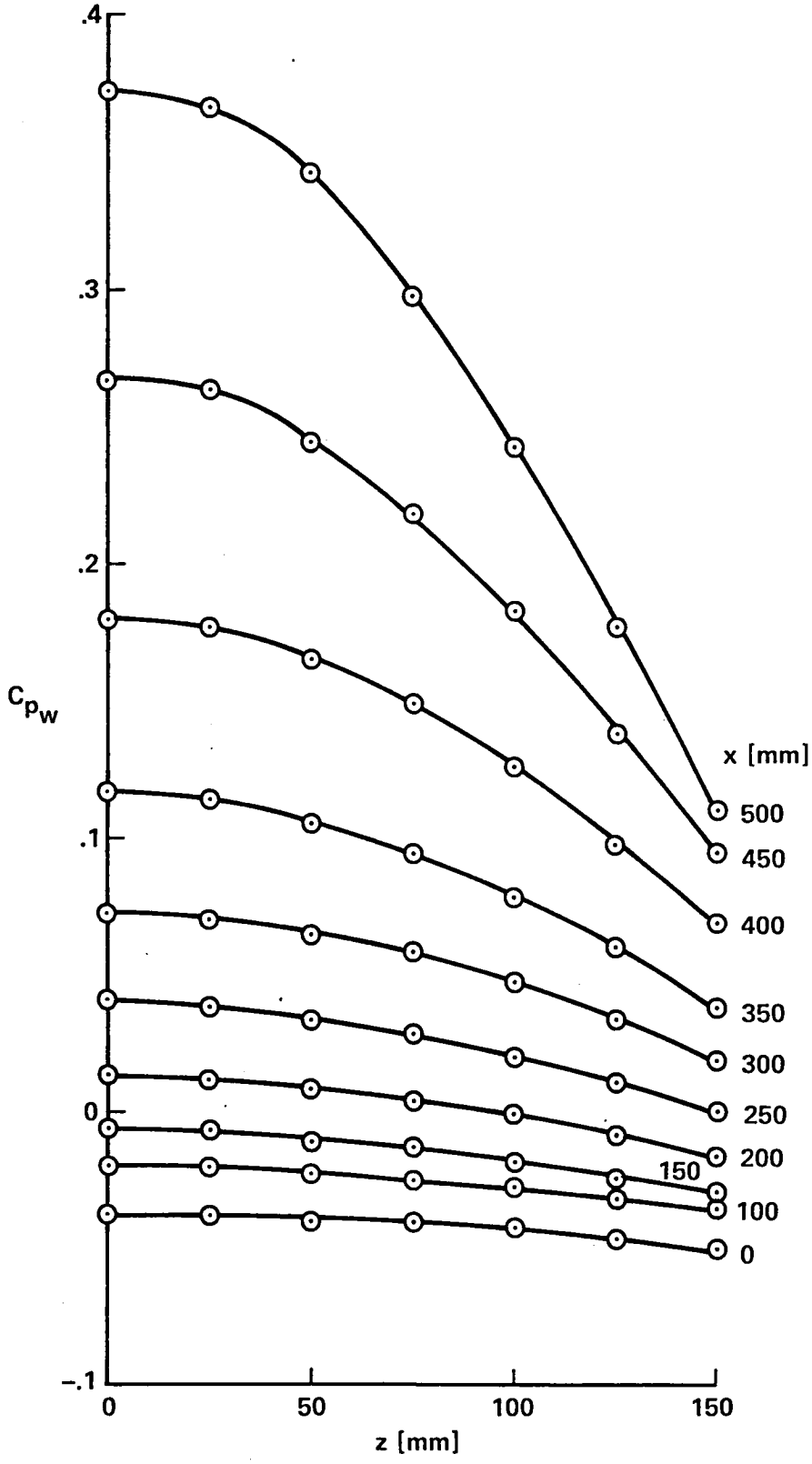

Figure 6. Measured wall pressure distribution

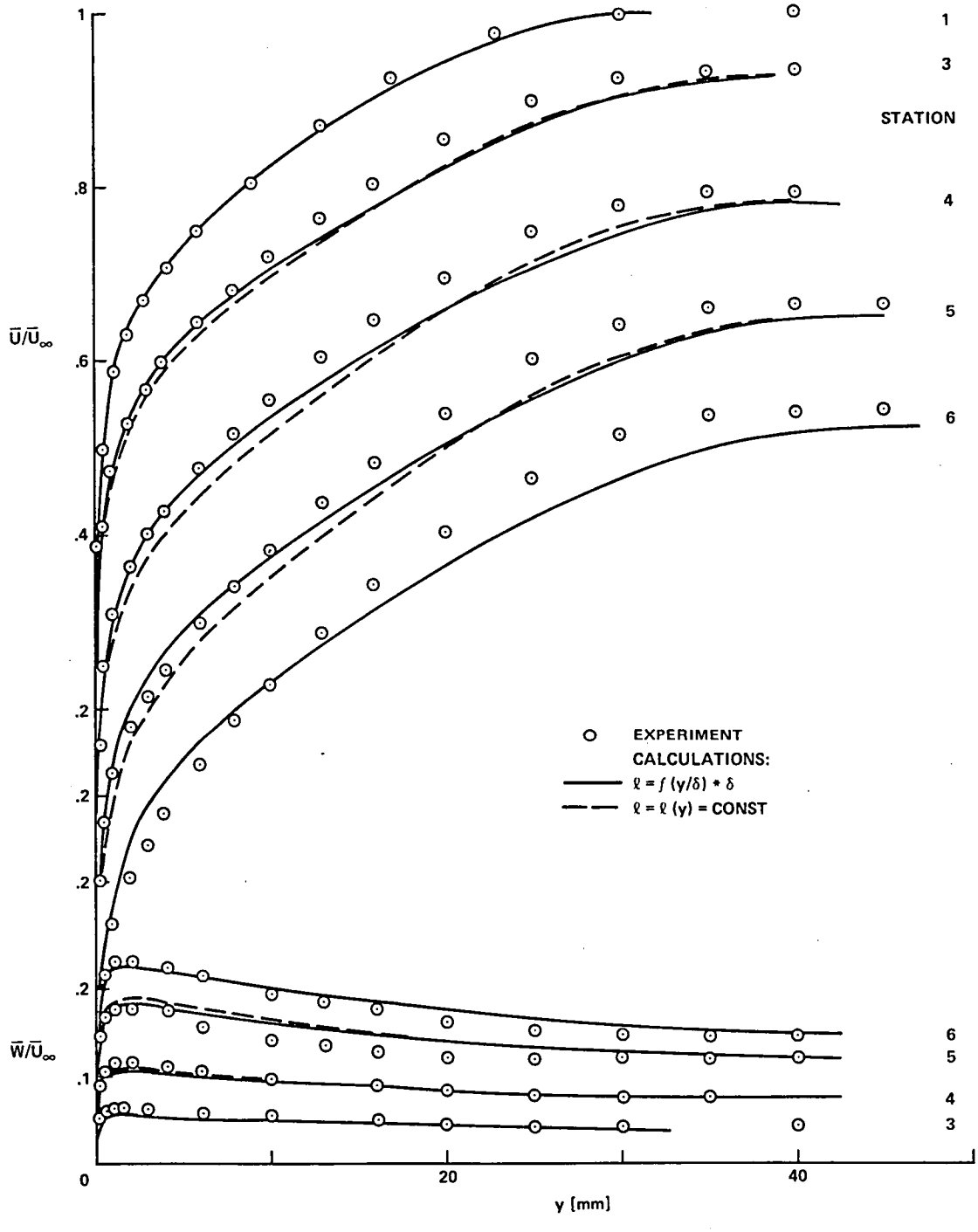

Figure 7. - Comparison of measured and computed mean velocities.

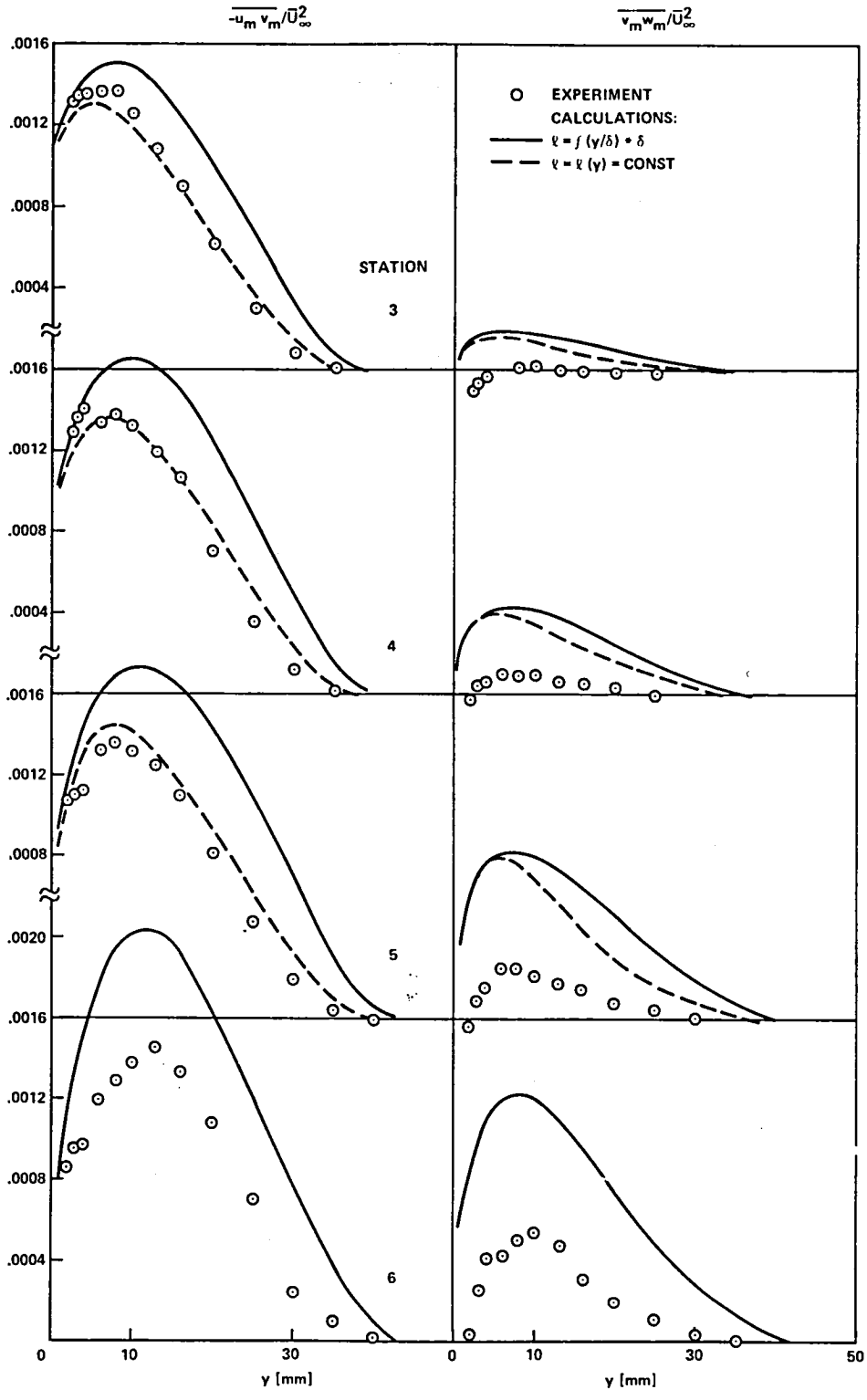

Figure 8. - Comparison of measured and computed Reynolds shear stresses.

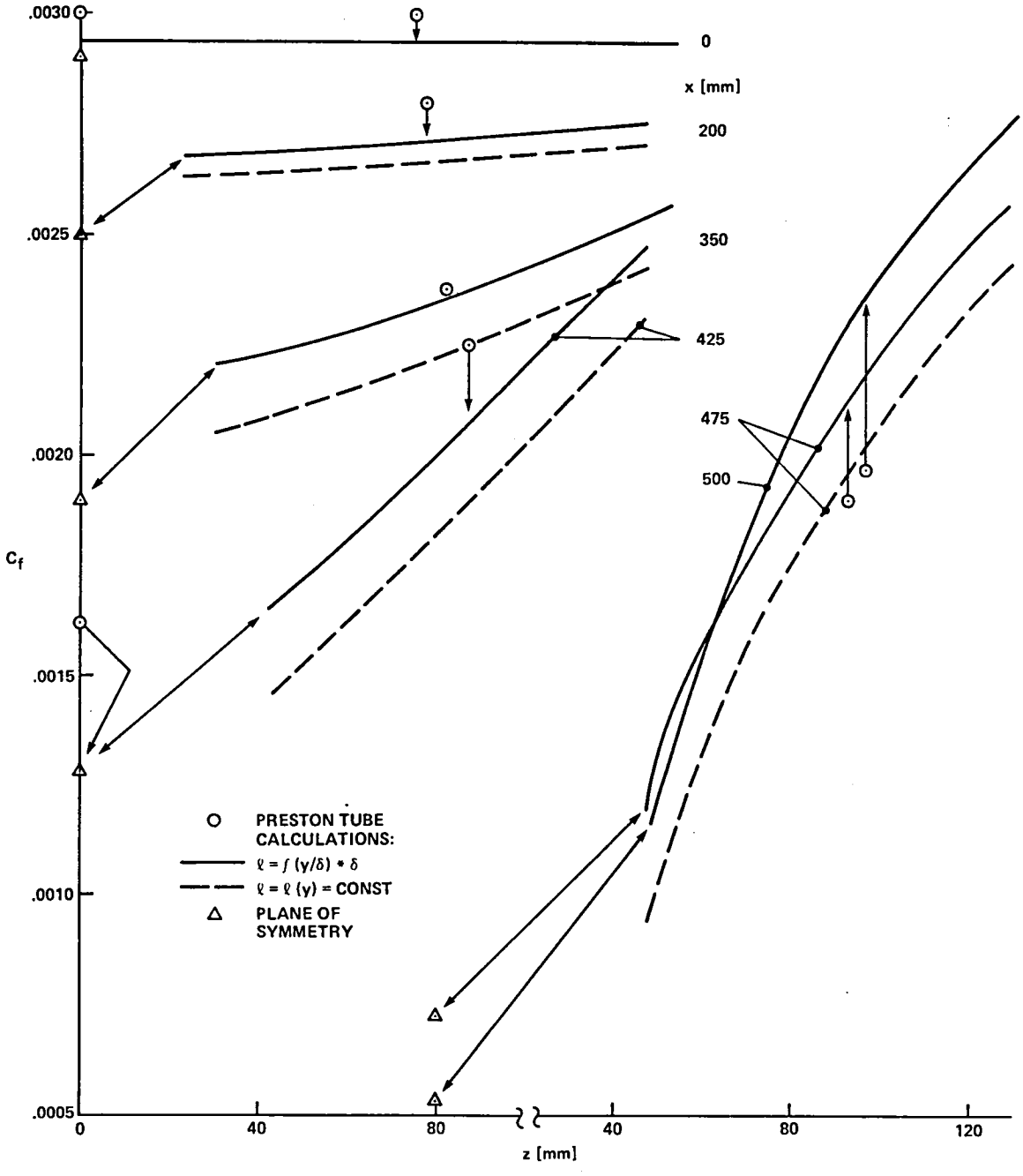

Figure 9. - Comparison of measured and computed skin friction coefficients.

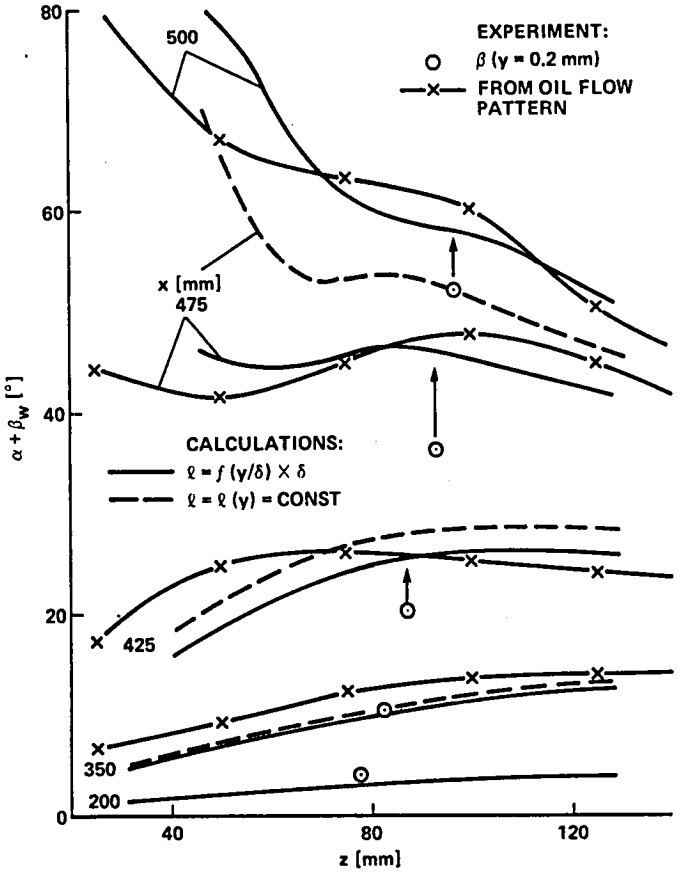

Figure 10. - Comparison of measured and computed wall turning angles.

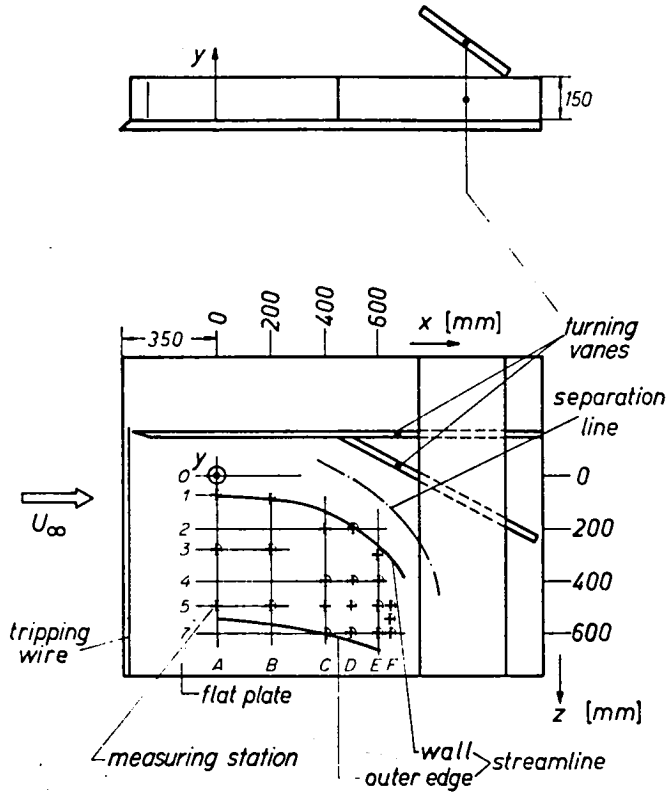

Figure 11. - Experimental setup of reference 3.

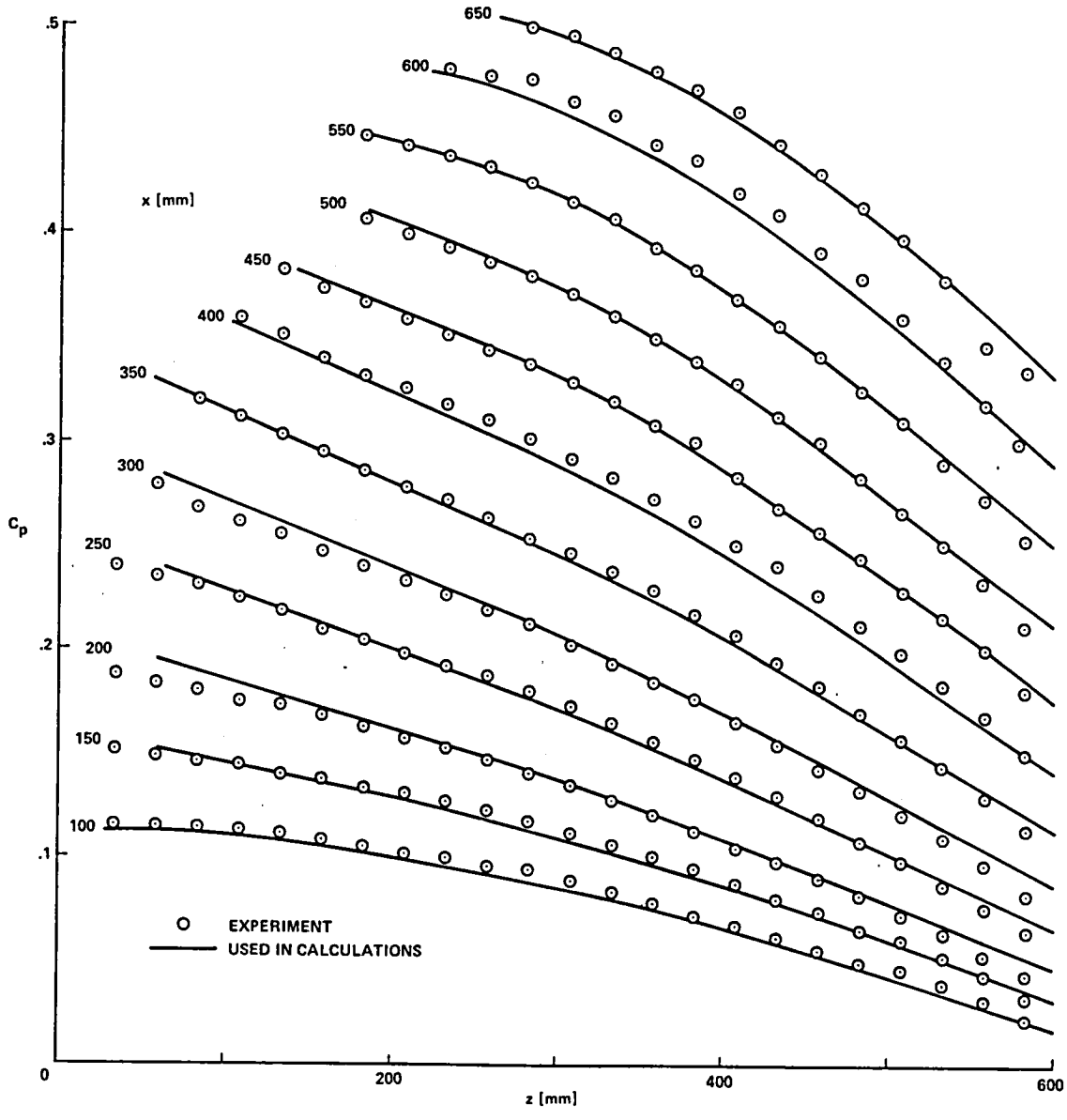

Figure 12. - Measured and smoothed pressure distribution.

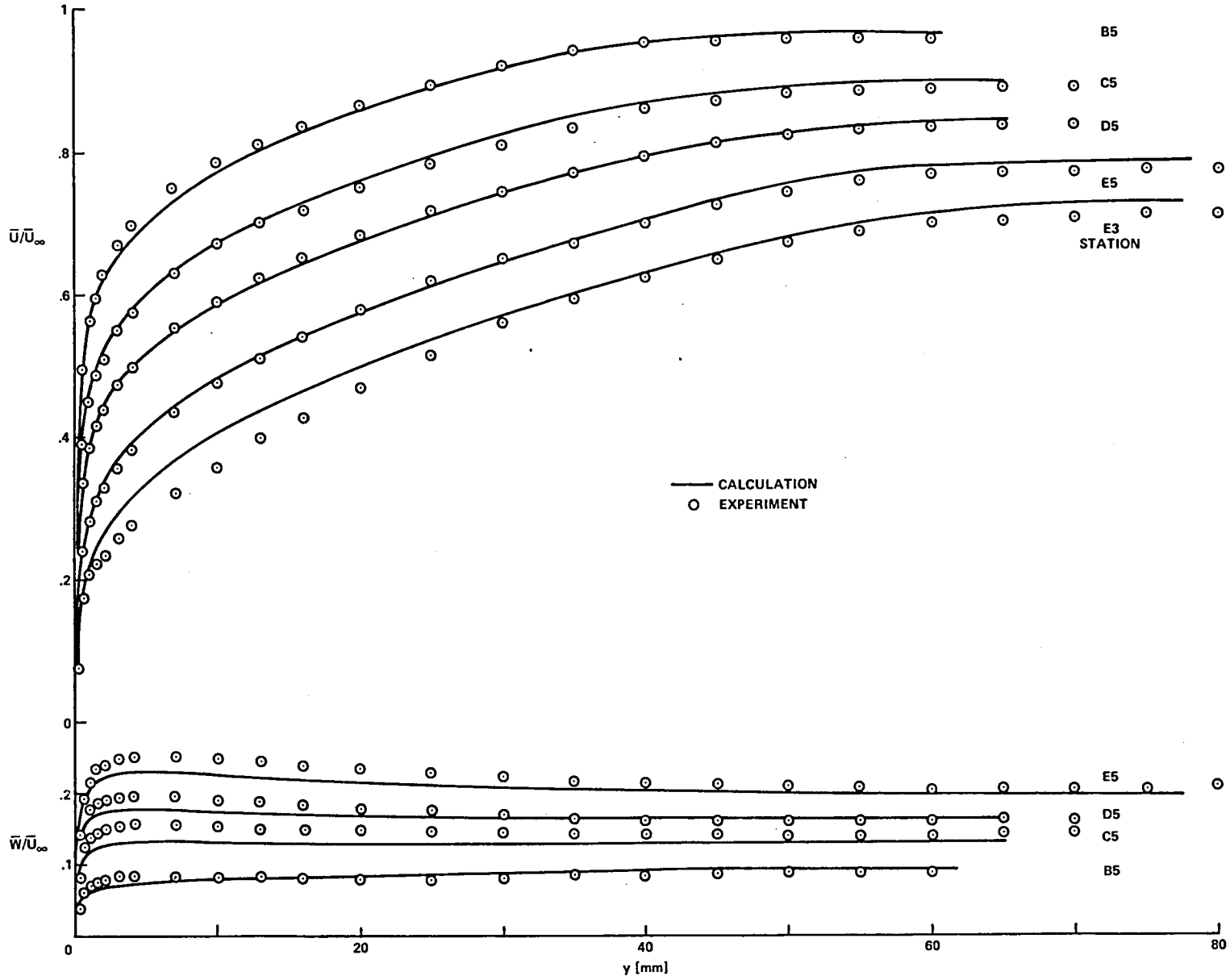

Figure 13. - Comparison of measured and computed mean velocities.

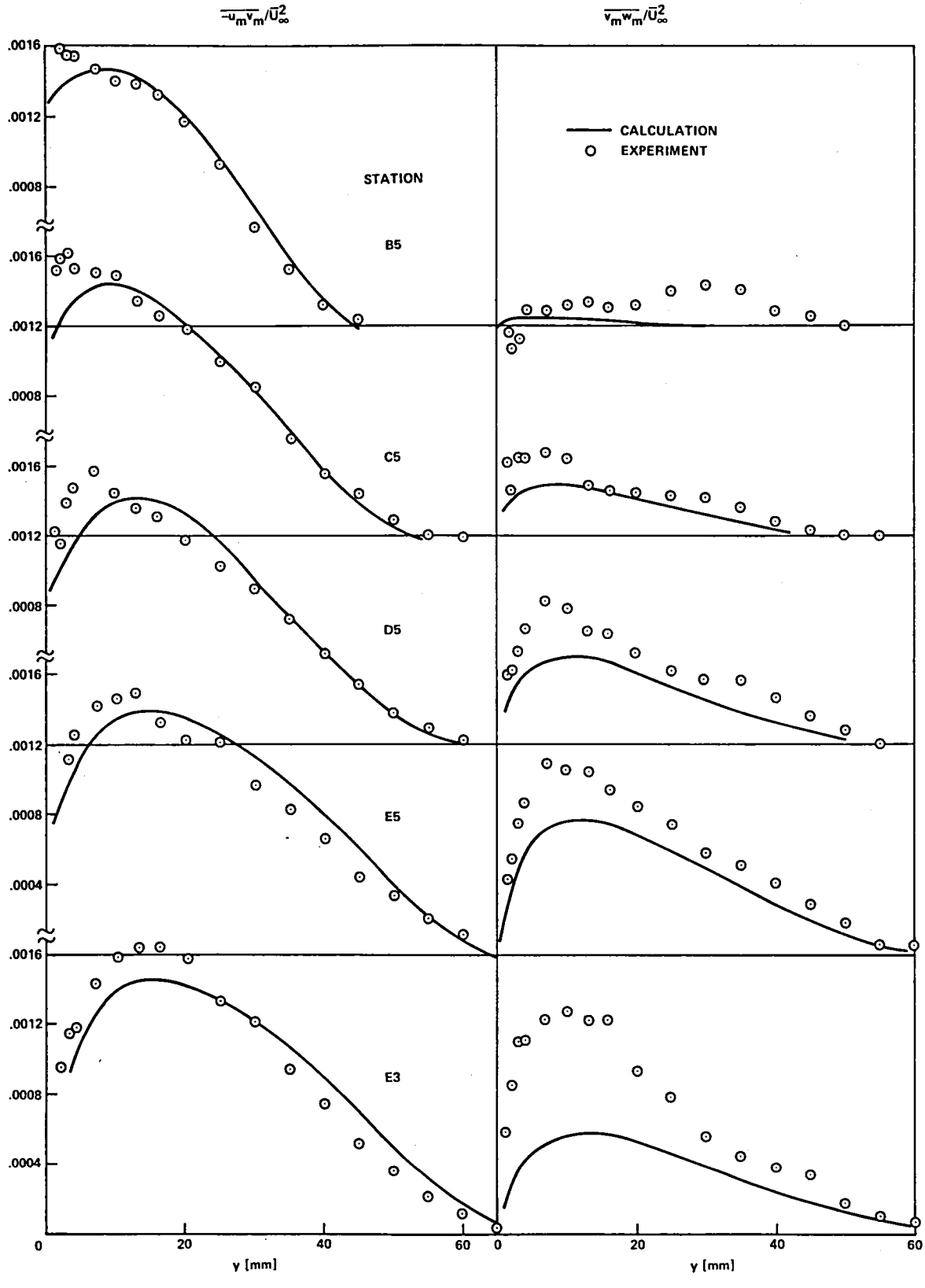

Figure 14. - Comparison of measured and computed Reynolds shear stresses.

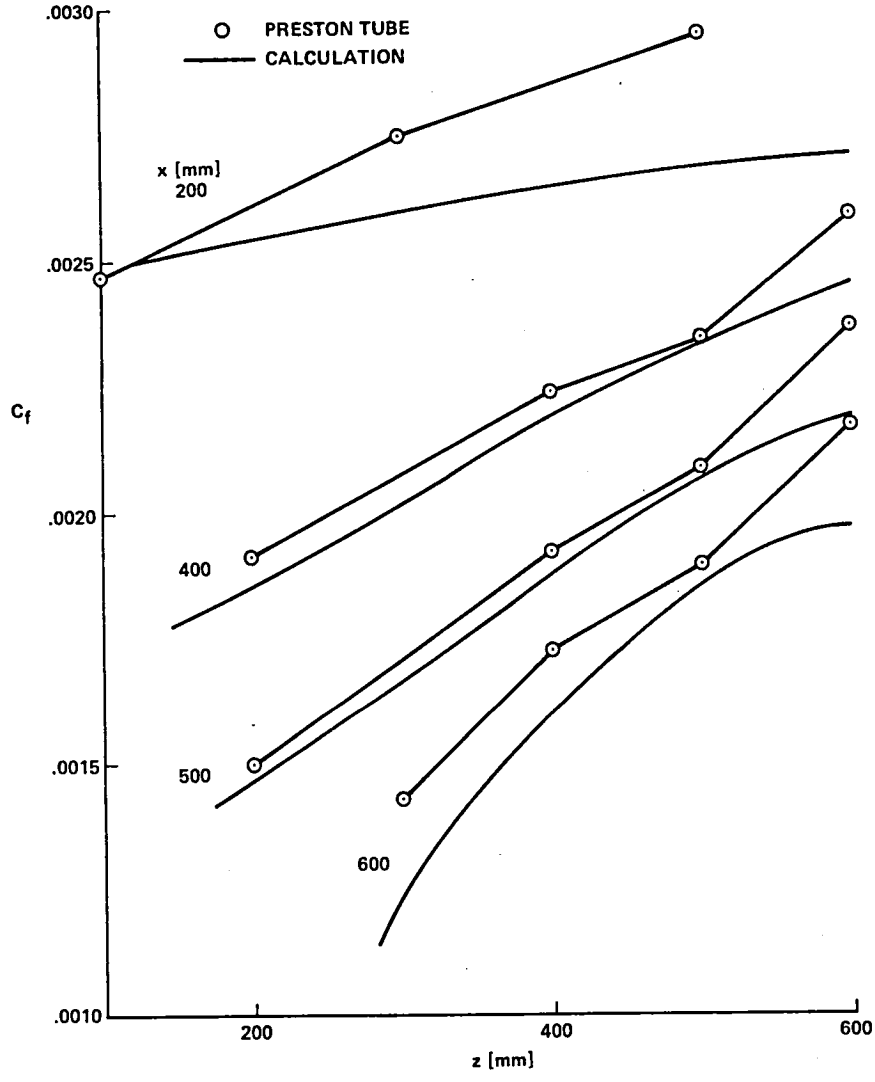

Figure 15. - Comparison of measured and computed skin friction coefficients.

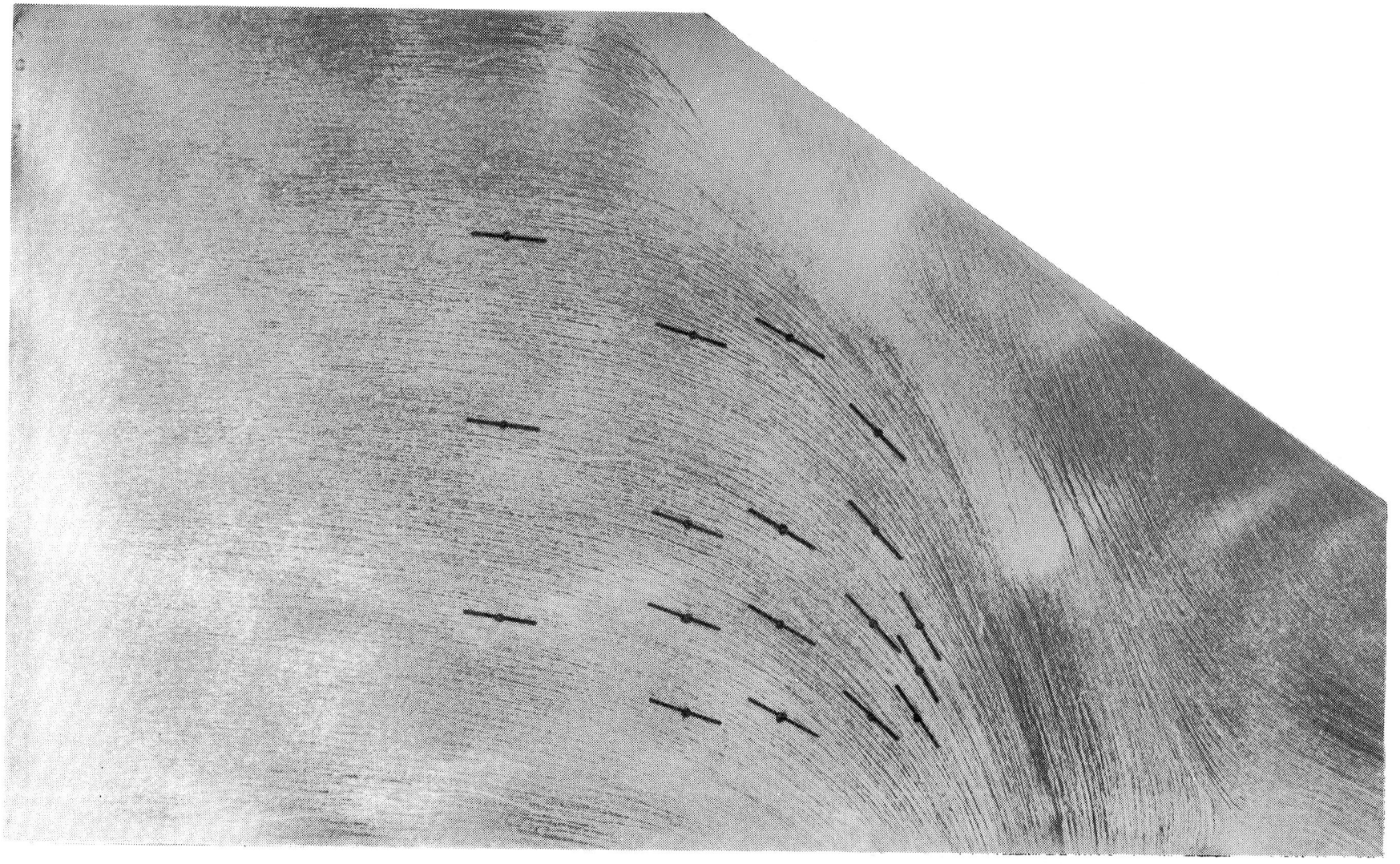

Figure 16. - Comparison of oil-flow pattern with wall-streamline directions computed at measuring stations.

1. Report No.	2. Government Accession No.	3. Recipient's Catalog No.
NASA TM 84230		

4. Title and Subtitle	5. Report Date
COMPUTATION OF INCOMPRESSIBLE, THREE-DIMENSIONAL TURBULENT BOUNDARY LAYERS AND COMPARISON WITH EXPERIMENT	May 1982
	6. Performing Organization Code
7. Author(s)	8. Performing Organization Report No.
Udo R. Müller	A-8873
	10. Work Unit No.
9. Performing Organization Name and Address	T-4219
NASA Ames Research Center Moffett Field, Calif. 94035	11. Contract or Grant No.
	13. Type of Report and Period Covered
12. Sponsoring Agency Name and Address	Technical Memorandum
National Aeronautics and Space Administration Washington, D.C. 20546	14. Sponsoring Agency Code

15. Supplementary Notes

Point of contact: Udo R. Müller, Ames Research Center, MS 229-1, Moffett Field, CA 94035. (415) 965-6192
FTS (448) 965-6192

16. Abstract

The incompressible three-dimensional, turbulent boundary layer (3DTBL) experiments of van den Berg and Elsenaar (ref. 1), Dechow (ref. 2) and Müller (ref. 3) were simulated numerically by integrating the boundary-layer equations together with an algebraic eddy-viscosity turbulence model. For the flow treated by van den Berg and Elsenaar, the downstream portion, where the crossflow was large, could not be predicted with the present computational method; we feel that this flow was significantly influenced by elliptic flow-field effects. Though Dechow's experiment also indicated departures from the boundary-layer concept, our calculations agreed reasonably well with the mean-flow development up to separation. In Müller's experiment the normal pressure gradients were found to be negligible in regions with large skewing and enabled us to test turbulence models using the boundary-layer equations. The simulation of this flow compared favorably with the experimental data throughout the flow field and suggested the applicability of algebraic eddy-viscosity models for 3DTBLs.

17. Key Words (Suggested by Author(s))	18. Distribution Statement
3-D Boundary Layers	Unlimited Subject Category – 34

19. Security Classif. (of this report)	20. Security Classif. (of this page)	21. No. of Pages	22. Price*
Unclassified	Unclassified	25	A02

*For sale by the National Technical Information Service, Springfield, Virginia 22161